Morphology control and field emission characteristics of carbon nanofibers grown by CVD

One-dimensional carbon nanostructures, such as carbon nanofibers, show outstanding field emission properties due to their high aspect ratio. Platelet and tubular carbon nanofibers were grown by Plasma Enhanced Chemical Vapor Deposition. The fiber morphology could be tailored to the desired geometry by selecting the growth pressure in the 20-200 Torr range and the growth temperature between 700 and 900 °C. Fowler-Nordheim field emission currents were measured by using the variable anode-cathode distance technique. The results showed that, although nanofibers with different morphology have similar emission characteristics – such as very low electric field threshold (lower than 2 V m-1) and high stable current density (hundreds of mA/cm^2) – a different behavior could be observed by a fine I-V curve analysis

Elena Salernitano, Theodoros Dikonimos Makris, Rossella Giorgi, Nicola Lisi, Serena Gagliardi, Maria Federica De Riccardis, Daniela Carbone, Emanuela Piscopiello, Stefano Carta, Gennaro Conte

Controllo della morfologia di nanofibre di carbonio sintetizzate mediante CVD e proprietà di emissione di campo

Le nanostrutture di carbonio monodimensionali, come le nanofibre, presentano proprietà di emissione di campo prominenti, dovute all'elevato rapporto di forma. Nanofibre di carbonio di morfologia "platelet" e tubolari sono state sintetizzate mediante Deposizione Chimica da fase Vapore assistita da plasma . La morfologia delle fibre può essere controllata selezionando in maniera opportuna la pressione di processo tra 20 e 200 Torr e la temperatura tra 700 e 900 °C. Le correnti Fowler-Nordheim di emissione di campo sono state misurate utilizzando il metodo della distanza anodo-catodo variabile. I risultati ottenuti hanno mostrato che, sebbene nanofibre con differenti morfologie abbiano caratteristiche di emissione simili, come la bassissima soglia di campo elettrico (inferiore a 2 V m-1) e l'elevata densità di corrente (centinaia di mA/cm^2), un diverso comportamento può essere evidenziato da un'accurata analisi delle curve I-V

Elena Salernitano, Theodoros Dikonimos Makris, Rossella Giorgi, Nicola Lisi, Serena Gagliardi
ENEA, Technical Unit for Material Technologies, Rome
Daniela Carbone, Maria Federica De Riccardis, Emanuela Piscopiello
ENEA, Technical Unit for Brindisi Material Technologies
Stefano Carta, Gennaro Conte
Roma Tre University, Solid State and Diamond Electronics Lab, Department of Physics, IFN-CNR and CNISM, Rome

Introduction

One–dimensional carbon nanomaterials, such as carbon nanotubes (CNTs) and carbon nanofibres (CNFs), exhibit excellent physical and chemical properties, due to their unique structure and high aspect ratio. Carbon nanofibers are commonly classified into different structural forms, depending on the angle that graphene layers form with the fiber axis [1]. In platelet CNFs (P-CNF), graphene layers are perpendicular to the filament axis; oriented at an angle between 50 and 70° in the herringbone CNFs (H-CNF) and parallel to the fiber axis in the tubular CNFs (T-CNF). Since the properties of graphite are anisotropic, graphene layers orientation strongly affects the resulting material properties such as electrical and thermal conductivity, mechanical strength and stiffness. It is worth noting that exercising control over the morphology and stacking layers of CNFs is of considerable importance for applications.

Several previous works reported on the key parameters determining the structure of carbon nanofibers grown by chemical vapor deposition (CVD) processes. The catalyst is thought to be responsible for the CNFs structure variation due to the metal particles evolution during the reaction [2-5].

During the process, distinct crystallographic faces are generated, some of which allowing the adsorbed carbon atoms to arrange into graphenes. A crucial role is assigned to the growth temperature since it affects the shape of the catalyst particles (faceted, spherical, etc.) and, consequently, the arrangement of carbon layers and the resulting nanofibers structure [6,7]. The formation of substructures (nanorods and nanoplates) working as building blocks during the CNFs growth process has been also observed [1]. The fibers appear to be formed by the assembling of these substructures and the final structure results from their arrangement and alignment. A further parameter reported as affecting CNFs morphology is the amount of hydrogen in the gaseous mixture [8-9]. The availability of enough hydrogen to satisfy free valences at the edges of graphite planes is thought to control the shape of CNFs. Hydrogen can terminate the highly energetic dangling bonds at the edges of the stacked graphite sheets stabilizing open carbon forms; otherwise carbon filaments self-arrange in the more stable closed tubular form.

A large variety of potential applications is reported for fibrous carbon nanostructures: tubular structures are required for their mechanical properties for applications in composite materials; hollow tubes for their exceptional electronic properties; platelet CNFs, which have many defects and relatively lower strength, are considered interesting for their large surface area available along one direction and numerous edges of graphite layers on the surface.

All one-dimensional carbon nanostructures are considered to be promising candidates for field emission display applications being high-intensity and high-efficiency sources of electrons, when oriented along the collection axis. On the other hand, the material morphology is expected to strongly influence the electron emission properties of such emitters. Indeed, it is expected that electron emission might be enhanced along carbon atoms at the end of a filament or through the lateral plane of a graphene platelet.

In the present work the morphology control of CNFs via the process parameters is shown. By varying both the growth temperature and pressure a transition from tubular to platelet carbon nanofibers has been observed. While the occurrence of a transition from multiwalled carbon nanotubes to nanofibers at varying the power of a plasma reactor has been already shown [10], and a change from platelet to tubular type according to the synthesis temperature has been also reported [7,11], the influence of the pressure on the fiber morphology has never been highlighted.

Field emission properties of T-CNFs and P-CNFs were investigated at room temperature using the well established variable anode-cathode distance method [12,13]. Both types of CNFs resulted excellent field emitters with very low electric field threshold (lower than 2 $V\mu m^{-1}$) and high stable current density (hundreds of mA/cm^2). In comparison with typical metallic emitters, CNFs showed excellent performances also without Spindt tips array structure.

Experimental

Substrate preparation

The CNFs growth substrates consisted of graphite paper disks (10 mm diameter 0.4 mm thickness), where

nickel clusters were electrodeposited according to a previously optimized procedure [14], here briefly reported. A solution of 0.5 M $NiCl_2 \cdot 6H_2O$ with de-ionized water was prepared and adjusted to pH=3 by suitable HCl addition. A strip of carbon paper was used as working electrode. The counter-electrode was a Pt wire and a Saturated Calomel Electrode (SCE) was used as reference, mounted in a Luggin capillary containing the Nickel solution prepared for the deposition. The voltammetric measurements and the potentiostatic experiments were performed by a PAR potentiostat model 273A, in remote control.

CNFs growth

The CNFs growth was performed into a "home built" original PECVD reactor (Patent N.RM2007A000614 - 26-11-2007), consisting of a vacuum sealed quartz chamber, coaxial to a tube furnace, containing the substrate support and a twin electrode system. The reactor design allows to activate a DC glow discharge plasma inside the hot zone of the quartz tube chamber and uses the reactor chamber itself as an electric break (figure 1).

The gaseous precursors were CH_4 and H_2 mixtures, in the fixed flow ratio 7:1, while the total flow varied from 240 to 480 sccm. The chamber was first pumped down to rotary pump vacuum, then the furnace was heated up to the process temperature in H_2 stream. A high voltage was then applied between the electrodes, and when stable in hydrogen, the gas flow was switched to the process gas mixture. A needle valve was preset in order to adjust the process pressure to the desired value. A voltage drop of 0.7-1 kV across the electrodes and a current of 45 mA were measured during the growth process. The process parameters were kept constant for 30 minutes. The process pressure was varied in the range between 20 and 200 Torr and the growth temperature in the range between 700 and 900 °C.

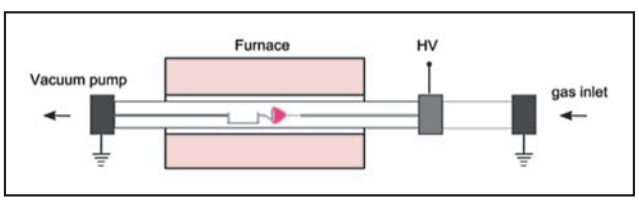

FIGURE 1 Scheme of the CVD reactor

Morphological and structural analysis

The substrates and the grown carbon nanofibers were analysed by a Field Emission Gun Scanning Electron Microscope (FEG-SEM LEO mod. 1530), equipped with a high-resolution secondary electrons detector (in-lens detector).

Structural investigations on the nanofibers were performed by using a Transmission Electron Microscope (TECNAI F30) operating at 300 kV and point-to-point resolution of 0.205 nm.

Field emission measurements

Field Emission (FE) tests were carried out at room temperature in vacuum conditions (10^{-4} Pa) by using variable anode to cathode distance method. A 5 mm diameter stainless steel spherical anode suspended over the flat sample was used to minimize the edge effects and avoid any misalignment problem. The sample holder was secured on a micrometer head with 0.1 μm resolution (Mitutoyo n1 10_102) which allowed the sample/anode distance to be finely controlled. A high resistance ammeter HP4339A was used to acquire the *I–V* characteristics. The maximum emission current was limited to 5×10^{-6} A in order to avoid sample damaging leading to morphology variations among succeeding measurements at different distances. Different regions were also tested to evaluate the material homogeneity. I-V measurements were carried out automatically decreasing the anode-cathode distance by succeeding 20 μm steps, by using a step motor and a program developed in Labview 7.

Results

CNFs growth

Plasma-assisted thermal decomposition of methane and hydrogen gaseous mixture in presence of Ni clusters was carried out to produce carbon nanofibres of different structure, by varying temperature, pressure and precursors mixture composition. A general view of typical samples with a dense mat of platelet and tubular CNFs types is reported in figure 2, where the high purity of both materials and the different curling

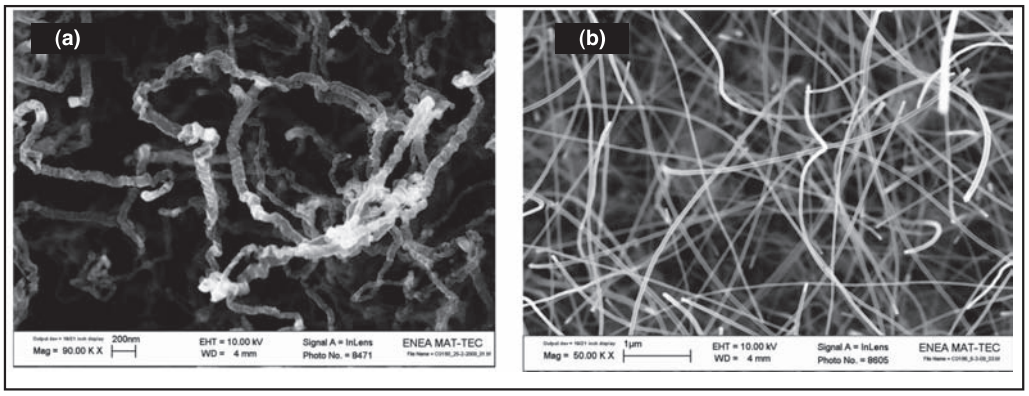

FIGURE 2

FEG-SEM micrograph of platelet (a) and tubular (b) CNFs

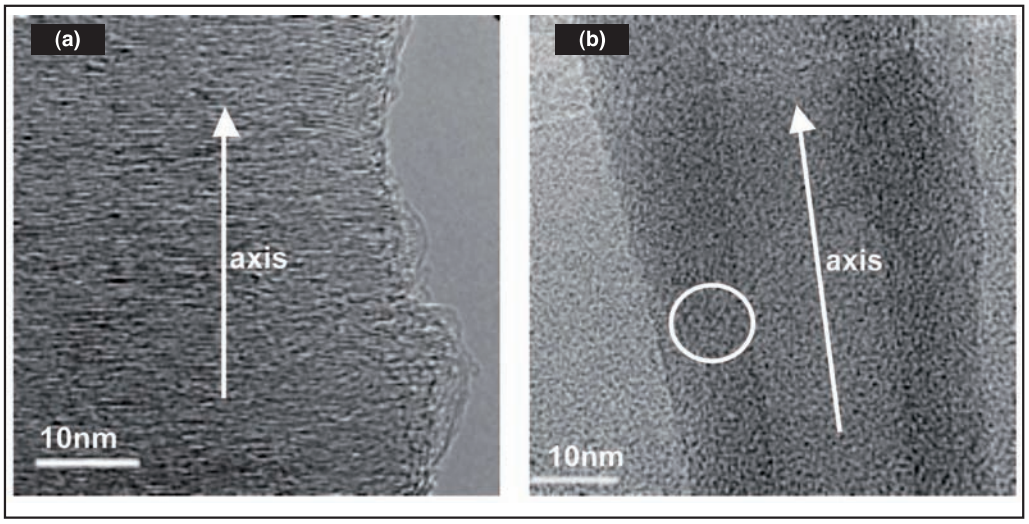

FIGURE 3

TEM images showing the structure of platelet (a) and tubular (b) CNFs

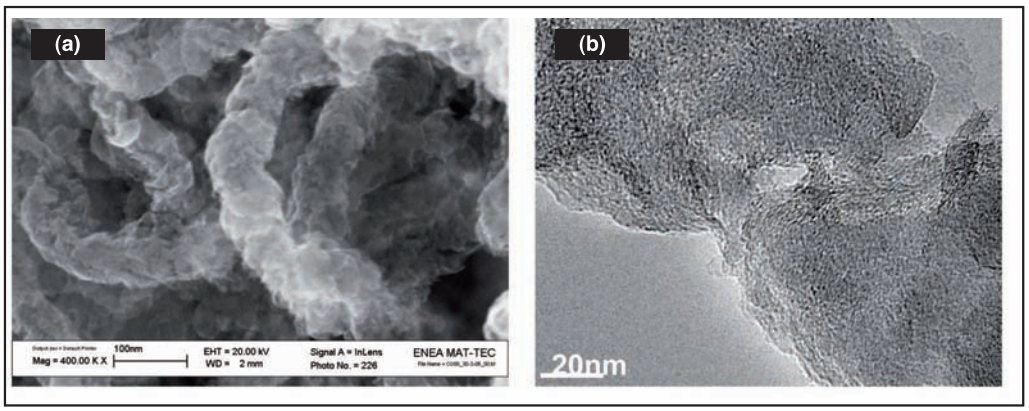

FIGURE 4

CNF with turbostratic structure: SEM (a) and High Resolution TEM (b) images

is evident. Higher magnification SEM analysis revealed that the nanofiber diameters were in the range of 100-120 nm for P-CNFs and in the range of 50-80 nm for T-CNFs. TEM analysis highlighted the different orientation of the graphene layers with respect to the fiber axis: perpendicular in P-CNFs and parallel in T-CNFs (figure 3).

Moreover, under certain conditions, as discussed be-

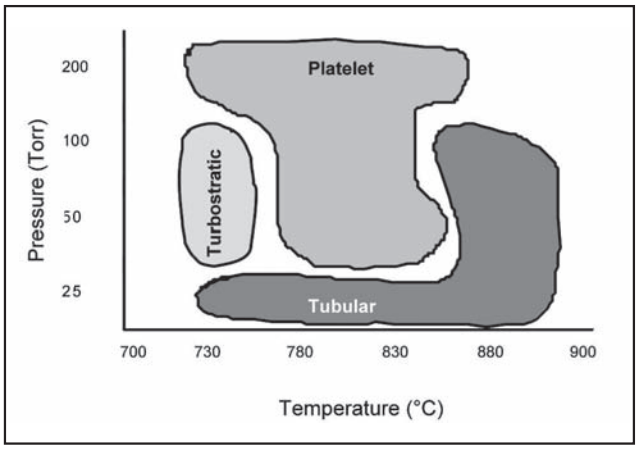

FIGURE 5 Qualitative phase diagram of CNFs morphologies

low, fibers with the turbostratic structure, where the graphene layers are randomly oriented, have been grown (figure 4). Other authors have reported the occurrence of this type of fibers [11].

The reaction temperature and pressure were found both as the process parameters affecting the alignment of the graphene layers with respect to the fiber axis. The pressure and temperature ranges studied were 20-200 Torr and 700-900 °C respectively. The experimental results can be summarized in a sort of phase diagram where the existence regions of the three CNFs morphologies are reported (figure 5).

It was found that the platelet morphology was predominant, independently of temperature, at the highest pressure (200 Torr); on the contrary, the tubular morphology was predominant, independently of temperature, at the lowest pressure (20 Torr); turbostratic structure was observed only at low temperature (730 °C) and at the intermediate pressure values (50 and 100 Torr). A transition from platelet to tubular CNFs was observed with a temperature increase from 780 to 880 °C, keeping the total pressure in the range between 35 and 100 Torr. At higher temperature (> 900 °C) no growth was observed, possibly due to the deactivation of the catalyst.

The temperature-dependent behavior was thought to be consistent with the hypothesis that the catalyst shape plays a crucial role in determining the orientation of the deposited graphene layers and, consequently, the angle between the stacked planes and the filament axis [6]. Indeed, SEM observation reported in figure 6 confirmed that, at low temperature, catalyst particles remained faceted or just softened and changed their shape from faceted to flat giving rise to platelet CNFs (panel a), whereas the increase in growth temperature determined a further metal particle softening, originating cylindrical catalyst particles and consequently tubular CNFs (panel b). A similar behavior of the catalyst particles with temperature has been hypothesized by other authors [7].

Understanding the effect of the total pressure on the CNFs morphology was less direct than temperature's, since a total pressure change means that several process conditions are affected, including the gas residence time in the reactor and the transit time through the plasma region. However, some basic mechanisms could be hypothesized. The total growth pressure mainly affected the hydrogen content in the reaction chamber. An increase in the hydrogen content along

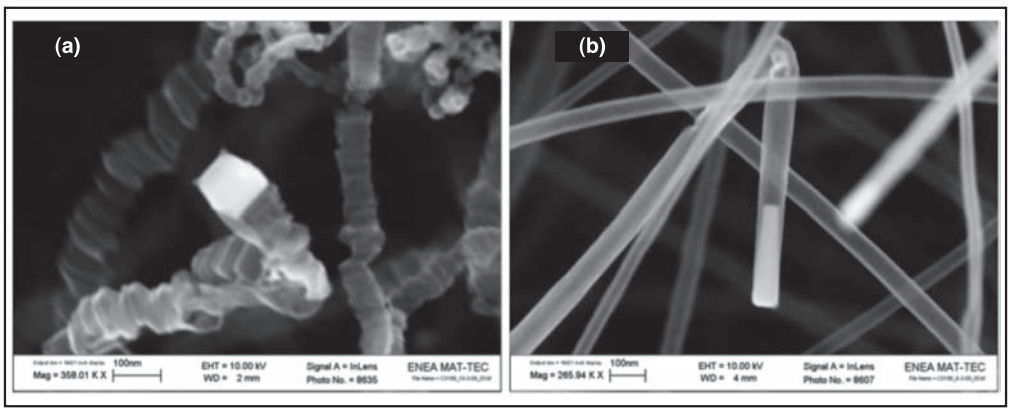

FIGURE 6
FEG-SEM micrograph showing the catalyst particle at the tip of platelet (a) and tubular (b) CNFs

with a pressure increase, even if the gas precursors ratio was kept constant, determined a higher availability of atomic hydrogen. According to previous works[9], a higher atomic hydrogen concentration is supposed to stabilize open graphene layers, terminating the dangling bonds at the edges of the stacked graphite sheets. Therefore, as pressure increased, the orientation angle between graphene layers and the fiber axis increased too, so that at 200 Torr only the platelet morphology was observed. At the lowest pressure (20 Torr), regardless of temperature, the only stable form found was the tubular structure, where the free valences were satisfied by bonding with catalyst surface or carbon atoms. It is worth noting that growth parameters and plasma parameters are interlinked, so that their effects on the CNF morphology could be hardly separated. Nevertheless, in order to separate the effect of temperature and pressure from that of the gas residence time in the reactor and of the transit time through the plasma region, some growths were performed by keeping the process parameters constant and varying the gas flow rates only. The total flow of the gaseous mixture was found to influence the density of the grown materials only, resulting in a denser mat gradually as the flow increased from 240 to 480 sccm, whereas the morphology was still determined by the growth parameters.

FE characteristics

The quantum mechanical theory of field emission was first published by R.H. Fowler and L. Nordheim (FN theory) in 1928 [15] for a metallic emitter. Their model states that the dependence of the emitted current on the local electric field F and the work function Φ is defined as $I \propto (F^2/\Phi) \exp(B\Phi^{3/2}/F)$, with $B = 6.83\times10^9$ Vm^{-1} $eV^{-3/2}$. With respect to the applied macroscopic field $E = V/d$, where V is the voltage applied between electrodes separated by a distance d, the local field F is enhanced by the factor β, $F = \beta \cdot E$. The field enhancement factor β takes into account the capability of the emitter to amplify the local field at its surface. Larger values of β correspond to more efficient field emitter. Manipulating the FN equation we obtain $\ln(I/V^2) = \ln(a-b)/V$, where a is a parameter depending both on the material properties and on the emitter device structure; b is just related to Φ and β according to the equation $b = B\Phi^{3/2}d/\beta$. Once evaluated the anode–cathode interspacing d and assigned a fixed value to the work function, known from other experiments, the field enhancement factor β can be calculated from the slope of the experimental I–V curve according to a linear fit. Another important feature of a field emitter is the macroscopic electric field threshold, E_{th}, defined as the minimum electric field necessary to obtain a fixed emission current I_{th} (in our case I_{th} = 100 pA). Lower values of E_{th} correspond to a better field emitter. In our experimental setup, variable anode-to-cathode distance method is used. The CNFs with different morphologies were characterized as field emitters in the same setup conditions. Starting from an unknown distance d_0 samples were moved towards the anode. I–V characteristics were recorded for each distance $d = d_0 - \Delta d$, where Δd is the performed displacement. Emitted current from platelet and tubular CNFs changed with applied voltage according to the FN expression.

Fowler-Nordheim emission from nanofibers with platelet morphology showed linear behaviour in FN plot and excellent spatial distribution of I-V curves for different micrometer distances as shows figure 7a. After an initial resistive behavior, for each distance, the current increased faster as the distance was decreased. An apparent saturation of the measured current was found at higher voltages. The FN plot is reported in figure 7b, where the expected linear relationship of the FN theory is observed over four orders of magnitude.

On the contrary, emission from nanofibers with tubular morphology seemed to be more disordered, as shown in figure 8. After the initial resistive trend, associated to the ohmic current leakage of the apparatus, the current started increasing faster for each tested distance, but an apparent current saturation was observed at intermediate voltage values, addressing the presence of an energy barrier, at least at room temperature. After each plateau, the current increased again with a different slope. This behaviour may be associated, in average, to emission sites with different angles with respect to the collection axis. Due to the entanglement of the nanofibers, the density of the emission sites (fiber tips) is supposed to be lower than for sample of platelet type, where the emission can originate also from the graphene edge along the walls of the fiber. On the other hand, it should be also considered that the external electric field applied to a

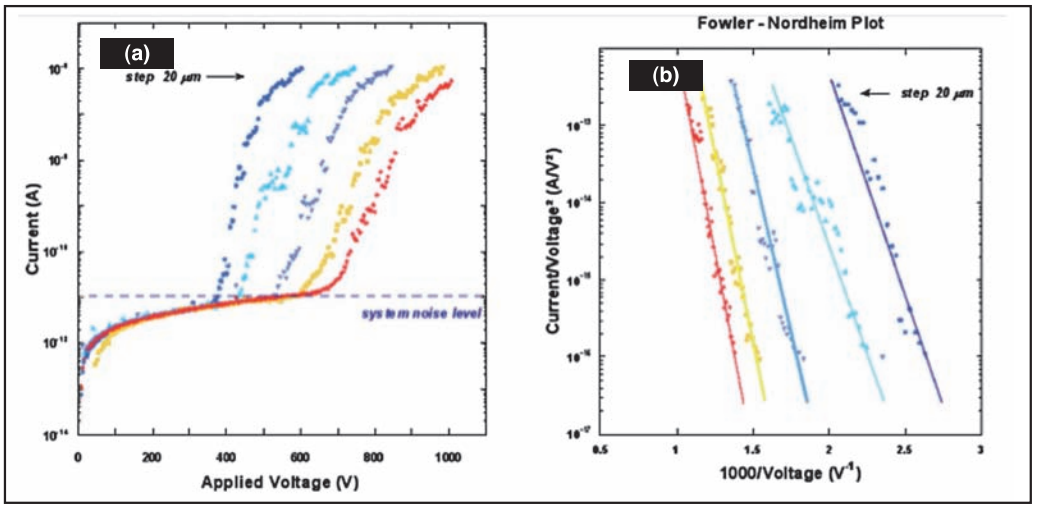

FIGURE 7 Field emission plots of platelet-type carbon nanofibres

semiconductor or insulating material induces a surface bandbending influencing the emission properties from the conduction band as stated by the Stratton theory [16]. Such bandbending for a surface with defects and electronic states filled with electrons inside the bandgap, as expected for structured nanomaterials like graphene, might have averaged emission properties. The F-N plot does not allow extrapolating distinct slopes, but only an average value.

The electric field threshold was initially evaluated from the slope of voltage-distance plot. With the anode-to-cathode procedure here adopted, it is not necessary to know the exact value of the sample-to-probe distance, but only their distance variations. Thus, if we report the current density as a function of the electrical field, the curve in figure 9 is obtained, which is the result of more

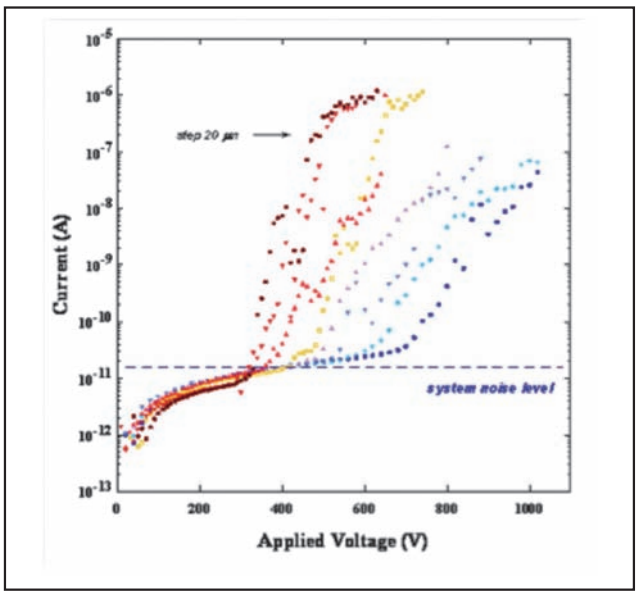

FIGURE 8 Field emission plots of tubular carbon nanofibres

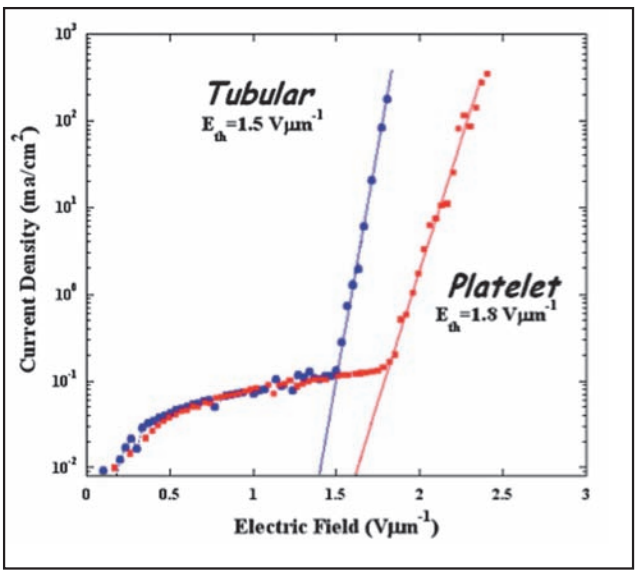

FIGURE 9 Comparison of E_{th} for different types of carbon nanofibres

overlapped curves. The platelet CNFs electric field threshold appears slightly higher than the tubular one, 1.8 $V\mu m^{-1}$ against 1.5 $V\mu m^{-1}$, and distinct slopes were observed, probably due to a different work function and/or to different enhancement factors of CNFs.
The contribution of the substrate to the total current emission was negligible. Evaluations on bare paper-graphite showed, in fact, that the emission began for applied voltage of 500 V at a distance of about 60 μm, and the electric field threshold was about 8.5 $V\mu m^{-1}$, nearly four times higher than for CNFs.
From the slope of F-N plots the field enhancement factor β was extrapolated. Values of $\beta \approx 390$ for platelet CNFs and $\beta \approx 450$ for tubular CNFs were obtained. Such quite similar values might be the result of the macroscopic morphology averaging, although fine structure differences in emission curves can be observed. Unlike the classical tip array structures, we could not correlate the enhancement factor to the geometrical arrangement of CNFs and, for this reason, so low values for β deserve a deeper investigation. Nevertheless, from the results it appears that CNFs with both morphologies can be considered as good emitters, able to sustain stable current density of the order of hundreds of mA/cm^2, while a slight better performance of the tubular type is evidenced by the lower E_{th} and the higher slope of the curve.

Conclusions

This work reports on the synthesis of carbon nanofibers with controlled morphology by methane and hydrogen mixture decomposition over Ni clusters in a plasma enhanced CVD reactor. The growth temperature and total pressure are shown to affect the orientation of the stacked graphene layers with respect to the fiber axis, giving rise to platelet and tubular morphology. The assembling of graphene sheets and the consequent fiber morphology was controlled in the growth pressure range between 20 and 200 Torr and in the growth temperature range between 700 and 900 °C. The growth mechanisms at the basis of the different carbon nanofibres are briefly discussed.
The field emission characteristics were studied. Slight differences of the energy threshold for field emission between the two types of nanofibers were observed. From the commercial point of view, materials used for flat panel displays should exhibit a field emission current density of $1 mA/cm^2$. Both platelet and tubular CNFs reached this value at 1.9 and 1.6 V/μm respectively. Therefore, the suitability of both CFNs types are confirmed, although a more in-depth study is mandatory to clarify the role of interface defects on the emission properties of such nanostructured materials.

References

[1] S.-H. Yoon, S. Lim, S.-H. Hong, W. Qiao, D.D. Whitehurst, I. Mochida, B. An, K. Yokogawa, *Carbon* 2005, 43, 1828.
[2] M.S. Kim, N.M. Rodriguez, R.T.K. Baker, *Journal of Catalysis* 1992, 134, 253.
[3] Y. Yang, H. Xu, W. Li, Nanotechnology 2005, 16, 129.
[4] R. Zheng, Y. Zhao, H. Liu, C. Liang, G. Cheng, Carbon 2006, 44, 742.
[5] N.M. Rodriguez, A. Chambers, R.T.K. Baker, *Langmuir* 1995, 11, 3862.
[6] A. Tanaka, S.-H. Yoon, I. Mochida, *Carbon* 2004, 42, 591.
[7] E. Tracz, R. Scholz, T. Borowiecki, *Applied Catalysis* 1990, 66, 133.
[8] P.E. Nolan, M.J. Schabel, D.C. Lynch, Carbon 1995, 33(1), 79.
[9] P.E. Nolan, D.C. Lynch, A.H. Cutler, J. Phys. Chem. B 1998, 102, 4165.
[10] L. Delzeit, I. Mc Aninch, B.A. Cruden, D. Hash, B. Chen, J. Han, M. Meyyappan, *J. Appl. Phys.* 2002, 91(9), 6027.
[11] Chao-Wei Huang, Hung-Chih wu, Wang-Hua Lin, Yuan-Yao Li, *Carbon* 2009,47, 795.
[12] S. Salvatori, E. Brugnoli, M.C. Rossi, F. Pinzari, *Diam. Relat. Mater.* 2001, 10, 852.
[13] R. Angelucci, R. Rizzoli, S. Salvatori, S. Nicoletti, A. Migliori, E. Brugnoli, *Appl. Surf. Sci.* 2002, 186, 423.
[14] M.F. De Riccardis, D. Carbone, Th. Dikonimos, R. Giorgi, N. Lisi, E. Salernitano, *Carbon* 2006, 44, 671.
[15] R.H. Fowler, L. Nordheim, *Proc. R. Soc.* 1928, 119, 173.
[16] R. Stratton Phys. Rev. 1962, 125, 67.